Synthesis of Double Side-Chain Liquid Crystalline Block Copolymers Using RAFT Polymerization and the Orientational Cooperative Effect

Yi Zhao, Bo Qi, Xia Tong, and Yue Zhao*

Département de chimie, Université de Sherbrooke, Sherbrooke, Québec, Canada J1K 2R1

Received January 6, 2008; Revised Manuscript Received March 17, 2008

ABSTRACT: We report on the synthesis and characterization of a new type of diblock copolymer that is composed of two side-chain liquid crystalline polymers (SCLCP1-*block*-SCLCP2). The diblock copolymer of poly{6-[4-(4-methoxyphenylazo)phenoxy]hexyl methacrylate}-*block*-poly{6-[4-(4-cyanophenyl)phenoxy]hexyl methacrylate} (PAzoMA-*b*-PBiPMA) was successfully synthesized using the reversible addition−fragmentation chain transfer (RAFT) polymerization. Low-polydispersity samples of various compositions can be prepared using either PAzoMA or PBiPMA macromolecular chain transfer agent. We show that the orientational cooperative effect can be effective even in microphase-separated samples due to the interaction of the two mesogens via the interface. Indeed, the photoinduced orientation of azobenzene groups on the PAzoMA block can bring biphenyl groups on the PBiPMA block to orient in the same direction inside their respective lamellar domains. While RAFT can be used to access to double or all-SCLC block copolymers, this study also demonstrates the potential interest of exploring the interplay of the LC order of different SCLCPs within a microphase-separated system.

Introduction

Among diblock copolymers, those composed of an amorphous and a side-chain liquid crystalline polymer (SCLCP) have attracted much attention because they display two levels of self-assembly and ordering.[1−11] The microphase separation-induced morphology, due to the immiscibility of the two blocks, can compete with the liquid crystalline (LC) order formed by the mesogenic side groups of the SCLCP. Many studies found that the morphology and the LC order can influence each other. For instance, Finkelmann et al.[8] showed that a chiral smectic phase of a SCLCP can promote the formation of the lamellar morphology that is accommodating for the layered smectic order; by contrast, if the microphase separation occurs in the isotropic phase of the SCLCP, a gyroid morphology is observed. As a further development, when the SCLCP contains azobenzene-based mesogens, new effects of interplay between the morphology, LC order, and photoisomerization can be generated. Examples include the decreased rate of photoorientation and photochemical LC order-to-disorder phase transition of azobenzene groups inside the confining microdomains[12] and the light-controlled alignment of cylindrical microdomains (formed by crystallizable poly(ethylene oxide)) related to the photoinduced orientation of azobenzene mesogens.[13]

This paper reports the synthesis and characterization of the first diblock copolymer built up from two SCLCPs, one of which contains azobenzene mesogenic side groups. The successful synthesis was carried out using the reversible addition−fragmentation chain transfer (RAFT) polymerization. We foresee that such double or all-SCLC block copolymers (SCLCP1-*block*-SCLCP2) might generate new features and properties. In addition to the interplay of the two-level self-assembly, the LC ordering of the different SCLCPs may also compete since the interface in the microphase-separated morphology is large and the motion and organization of LC molecules is cooperative. We synthesized poly{6-[4-(4-methoxyphenylazo)phenoxy]hexyl methacrylate}-*block*-poly{6-[4-(4-cyanophenyl)phenoxy]hexyl methacrylate} (Scheme 1), denoted as PAzoMA-*b*-PBiPMA or PBiPMA-*b*-PAzoMA depending on the order of polymerization of the two monomers. The use of PAzoMA renders this double SCLC block copolymer photoactive and enables us to investigate the orientational cooperative effect in this new type of block copolymer. The synthesis of diblock copolymers with one amorphous polymer and one azobenzene SCLCP can readily be accomplished using both atom transfer radical polymerization (ATRP)[12−16] and RAFT.[17,18] However, our earlier attempts at using ATRP to synthesize azobenzene-containing double SCLC block copolymers failed (only a few azobenzene monomeric units could be obtained). RAFT polymerization provides an efficient way to synthesize double or all-SCLC block copolymers that can be studied to reveal the even richer competition scenarios between LC order, morphology, and functionality than what is known so far with the amorphous polymer-*block*-SCLCP system.

Experimental Section

1. Synthesis. *Materials.* Anhydrous anisole (Aldrich, 99.7%), phenylmagnesium bromide solution (Aldrich, 1.0 M in tetrahydrofuran), and carbon disulfide (Aldrich, 99% anhydrous) were used as received. 2,2′-Azobis(isobutyronitrile) (AIBN) (Polysciences) was recrystallized twice from ethanol before use. Literature methods were utilized to synthesize the monomer with an azobenzene group, 6-[4-(4-methoxyphenylazo)phenoxy]hexyl methacrylate (AzoMA),[19] and the monomer with a biphenyl group, 6-[4-(4-cyanophenyl)phenoxy]hexyl methacrylate (BiPMA).[20] The starting chain transfer agent (CTA), 2-(2-cyanopropyl)dithiobenzoate (CPDB), was synthesized using a literature method.[21]

Synthesis of Macromolecular Chain Transfer Agents. The synthetic route to the diblock copolymer with two SCLCPs is shown in Scheme 1. Here the macromolecular chain transfer agent PAzoMA-CTA is first obtained through RAFT polymerization of the monomer using CPDB; it is then used to polymerize BiPMA to yield the diblock copolymer PAzoMA-*b*-PBiPMA. As will be shown later, the order of polymerization of the two monomers could be reversed by making first the macromolecular chain transfer agent PBiPMA-CTA, followed by the polymerization of AzoMA. In the latter case, the diblock copolymer will be denoted as PBiPMA-*b*-PAzoMA to reflect the difference in synthesis. What follows is a typical preparation for the macromolecular CTA. AzoMA (1.19 g, 3 mmol), AIBN (3.3 mg, 0.02 mmol), and CPDB (13 mg, 0.06 mmol) were added into a 10 mL one-necked flask, followed by the addition of 3 mL of anisole. After the solution under stirring was purged by nitrogen flow for 15 min, the flask was sealed and placed into an oil bath for reaction at 75 °C for 4 h. During the polymerization, a small amount of the sample was collected at various

* Corresponding author. E-mail: yue.zhao@usherbrooke.ca.

10.1021/ma8000302 CCC: $40.75
Published on Web 05/07/2008

Scheme 1. Synthetic Route to the Diblock Copolymer Composed of Two Side-Chain Liquid Crystalline Polymers That Contain Azobenzene and Biphenyl Mesogenic Groups[a]

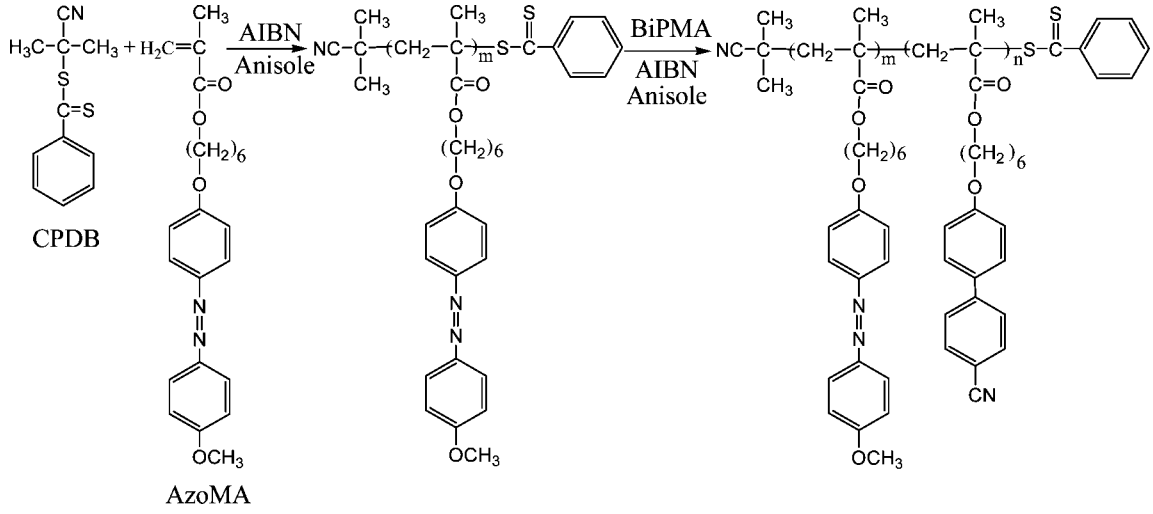

[a] CPDB = 2-(2-cyanopropyl)dithiobenzoate; AzoMA = 6-[4-(4-methoxyphenylazo)phenoxy]hexyl methacrylate; BiPMA = 6-[4-(4-cyanophenyl)phenoxy]hexyl methacrylate; AIBN = 2,2′-azobis(isobutyronitrile).

reaction times for the gel permeation chromatography (GPC) and ^{1}H NMR measurements. At the end of the reaction, the product was purified by precipitation from a dilute dichloromethane solution into petroleum ether (boiling point: 30−60 °C); this was repeated three times. The obtained PAzoMA-CTA was dried in a vacuum oven at room temperature for 24 h before use. ^{1}H NMR (300 MHz, δ ppm, $CDCl_3$): 7.83 (s, 4H, *o*-Ar *H* to −N═N−), 7.44 (b, 1H, *p*-Ar *H* to CSS), 6.94 (s, 4H, *m*-Ar *H* to −N═N−), 3.95 (s, 4H, OCH_2), 3.84 (s, 3H, OCH_3), 1.2−2.0 (m, 10H, $OCH_2CH_2CH_2$-$CH_2CH_2CH_2O$ and main chain CH_2), 0.8−1.1 (d, 3H, main chain CH_3). We found that the monomer conversion should be less than 50% in order to have PAzoMA-CTA effective in polymerizing the monomer of BiPMA. Basically the same experimental conditions were used to prepare the other macromolecular chain transfer agent, PBiPMA-CTA. ^{1}H NMR (300 MHz, δ ppm, $CDCl_3$): 7.84 (s, 2H, *o*-Ar *H* to CSS), 7.40−7.72 (t, 6H, *o,m*-Ar *H* to CN and *m*-Ar *H* to OCH_2), 6.90 (s, 2H, *o*-Ar *H* to OCH_2), 3.95 (s, 4H, OCH_2), 1.2−2.0 (m, 10H, $OCH_2CH_2CH_2CH_2CH_2CH_2O$ and main chain CH_2), 0.8−1.1 (d, 3H, main chain CH_3).

Synthesis of Diblock Copolymers. The double SCLC block copolymers were synthesized through the RAFT chain extension reaction using the macromolecular CTA, either PAzoMA-CTA for the growth of the second block of PBiPMA or PBiPMA-CTA for the growth of the PAzoMA block. An example of reaction is as follows: 6-[4-(4-cynophenyl)phenoxy]hexyl methacrylate (BiPMA) (54.5 mg, 0.15 mmol), AIBN (0.4 mg, 0.0025 mmol), and $PAzoMA_{34}$-CTA (105 mg, 0.0075 mmol) were added into a 5 mL one-necked flask. Then anhydrous anisole (0.5 mL) was added to dissolve the mixture. After 15 min nitrogen purge, the flask was sealed and placed in a preheated oil bath. The reaction was conducted at 75 °C for 4 h before the flask was put into liquid nitrogen to halt the reaction. The reaction solution was diluted with dichloromethane (3 mL) and was dripped into petroleum ether (250 mL) for precipitation of the product. This purification procedure was repeated three times, and the collected sample was dried in a vacuum oven for 24 h at room temperature. In this example, the diblock copolymer obtained is $PAzoMA_{34}$-*b*-$PBiPMA_{17}$. ^{1}H NMR (300 MHz, δ ppm, $CDCl_3$): 7.83 (s, 4H, *o*-Ar *H* to −N═N−), 7.40−7.72 (t, 6H, *o,m*-Ar *H* to CN and *m*-Ar *H* to OCH_2 in biphenyl), 6.80−6.94 (s, 6H, *o*-Ar *H* to OCH_2 in biphenyl and *m*-Ar *H* to −N═N−), 3.95 (s, 8H, OCH_2), 3.84 (s, 3H, OCH_3), 1.2−2.0 (m, 20H, $OCH_2CH_2CH_2CH_2CH_2CH_2O$ and main chain CH_2), 0.8−1.1 (d, 6H, main chain CH_3).

2. Characterizations. ^{1}H NMR spectra were recorded on a Bruker AC 300 spectrometer (300 MHz) using deuterated chloroform as solvent and tetramethylsilane as internal standard. The number- and weight-average molecular weights, M_n and M_w, were measured using a Waters gel permeation chromatograph (GPC) instrument equipped with a Waters 410 differential refractometer detector and a Waters 996 photodiode array detector. The measurements were made at 35 °C using one column (Waters Styragel HR4E, 7.8 mm × 300 mm, 5 μm beads). Polystyrene (PS) standards were used for the calibration and tetrahydrofuran (THF) as the eluent (flow rate: 1.0 mL min^{-1}). A Perkin-Elmer DSC-7 differential scanning calorimeter (DSC) was used to investigate the phase transition behaviors, using indium as the calibration standard and a heating or cooling rate of 10 °C min^{-1}. Glass transition temperatures (T_g's) were taken as the midpoint of the change in heat capacity. Polarizing optical microscopic (POM) observations were conducted on a Leitz DMR-P microscope equipped with an Instec hot stage. UV−vis spectra were recorded with a Varian 50 Bio spectrophotometer. X-ray diffraction (XRD) measurements were carried out using a Bruker diffractometer (D8 Discover) equipped with a Bruker AXS two-dimensional wire-grid detector (Cu Kα radiation λ = 1.542 Å). To record the diffraction patterns, the sample was filled into a capillary tube (1 mm diameter), and the sealed tube was placed in an Instec hot stage for temperature control. Tapping-mode atomic force microscopy (AFM, Nanoscope IV) was utilized to examine the morphology of thin block copolymer films spin-coated on silicon wafer from a toluene solution. For the photoisomerization and photoinduced orientation measurements, block copolymer films were exposed to UV or visible light using a spot curing system (Novacure 2100) combined with interference filters (10 nm bandwidth, Oriel). For photoinduced orientation, the intensity of unpolarized UV light (λ = 360 nm) was about 85 mW cm^{-2} and that of polarized visible light (λ = 440 nm) was 5 mW cm^{-2}. Prior to all experiments, except those using block copolymer solutions, samples were annealed at 140 °C (above the clearing temperature of SCLCPs) for 24 h to ensure the occurrence of microphase separation.

Results and Discussion

1. Syntheses and Characterization. For the two types of macromolecular chain transfer agents, PAzoMA-CTA and PBiPMA-CTA, different molecular weights were prepared and successfully used to make the double SCLC block copolymers. However, for the sake of clarity, only the results obtained with one PAzoMA-CTA and one PBiPMA-CTA will be presented and discussed in this paper. Prior to the synthesis of diblock copolymers, the controlled character of PAzoMA-CTA and PBiPMA-CTA initiated polymerization was investigated by

chain extension reactions with the same monomer, resulting in PAzoMA and PBiPMA homopolymers, respectively. For instance, for the chain extension reaction of PAzoMA at 75 °C, the polymer molecular weight (M_n, GPC) increased linearly with the monomer conversion up to 90%, with the polydispersity index (PDI = M_w/M_n, GPC) remaining below 1.15; there is, however, an inhibition period of about 40 min.[18]

The controlled growth of the second SCLCP block and the low polydispersity can be observed from GPC measurements. Figure 1 presents the results obtained using PAzoMA-CTA of $M_n = 1.38 \times 10^4$ (GPC) to prepare the diblock copolymer of PAzoMA-*b*-PBiPMA. Figure 1a shows the evolution of the GPC curve as a function of the reaction time at 75 °C for one molar feed ratio: [BiPMA]:[AIBN]:[PAzoMA-CTA] = 60:1:3. The peak appears at shorter elution times with increasing the reaction time up to 4 h and remains monomodel with almost no change in the width. Indeed, the low polydispersity index of 1.14 is virtually unchanged. This result clearly indicates a controlled growth of the second PBiPMA block via RAFT polymerization. Figure 1b shows the GPC curves of a series of block copolymers obtained by changing the BiPMA monomer concentration while keeping all other conditions the same (after 4 h reaction). As expected, the molecular weight of the PBiPMA block increases with increasing monomer concentration. However, at higher monomer concentrations, the peak becomes slightly less symmetrical, which is reflected by the increase of PDI to above 1.2. Figure 1c shows the plots of M_n(GPC) vs the BiPMA monomer conversion as determined by ^{1}H NMR and GPC, along with the corresponding change in PDI, for all the four feed ratios used. A linear fitting of the data can be obtained at low monomer concentrations (30:1:3 and 60:1:3), which is evidence of controlled growth of the PBiPMA block. However, the plots for higher monomer concentrations (120:1:3 and 180:1:3) appear to deviate from the linearity at high conversion degrees, which is accompanied by an increase in PDI. Here we note that the GPC results presented were obtained using a photodiode array detector by placing the absorption wavelength at 356 nm, which is the maximum absorption of azobenzene groups in the stable trans form. Similar results (with slightly smaller PDI) were obtained using the refractive index detector.

The same diblock copolymer can also be prepared in the reversed order, using PBiPMA-CTA to polymerize the AzoMA monomer. Figure 2 shows the GPC results using PBiPMA-CTA of $M_n = 1.01 \times 10^4$ to grow the second block of PAzoMA at 75 °C. In this case, the absorption wavelength of the photodiode array detector was set at 296 nm, which is about the absorption maximum of biphenyl groups. Figure 2a shows how the GPC curve changes over the reaction time up to 3 h for the molar feed ratio of [AzoMA]:[AIBN]:[PBiPMA-CTA] = 120:1:3, Figure 2b compares the GPC curves obtained after 3 h of reaction for various feed ratios, while Figure 2c shows the plots of M_n as a function of monomer conversion and the corresponding PDI. Basically, the same observations can be made regarding the controlled character of the polymerization. Nevertheless, it can be noticed that compared to the use of PAzoMA-CTA the increase in PDI occurs at relatively lower conversions. As already mentioned, more diblock samples were prepared using both PAzoMA-CTA and PBiPMA-CTA of different molecular weights. In all cases, RAFT was found to be effective to produce the double SCLC block copolymer, in contrast to our previous attempts using ATRP. However, in order to obtain an effective growth of the second block, the monomer conversion in preparing the macromolecular CTA should be kept to below 50% to limit the possible coupling termination reactions.

Table 1 lists the characteristics of the two series of diblock copolymers discussed above. The reported block copolymer compositions were obtained as follows. The M_n(GPC) of

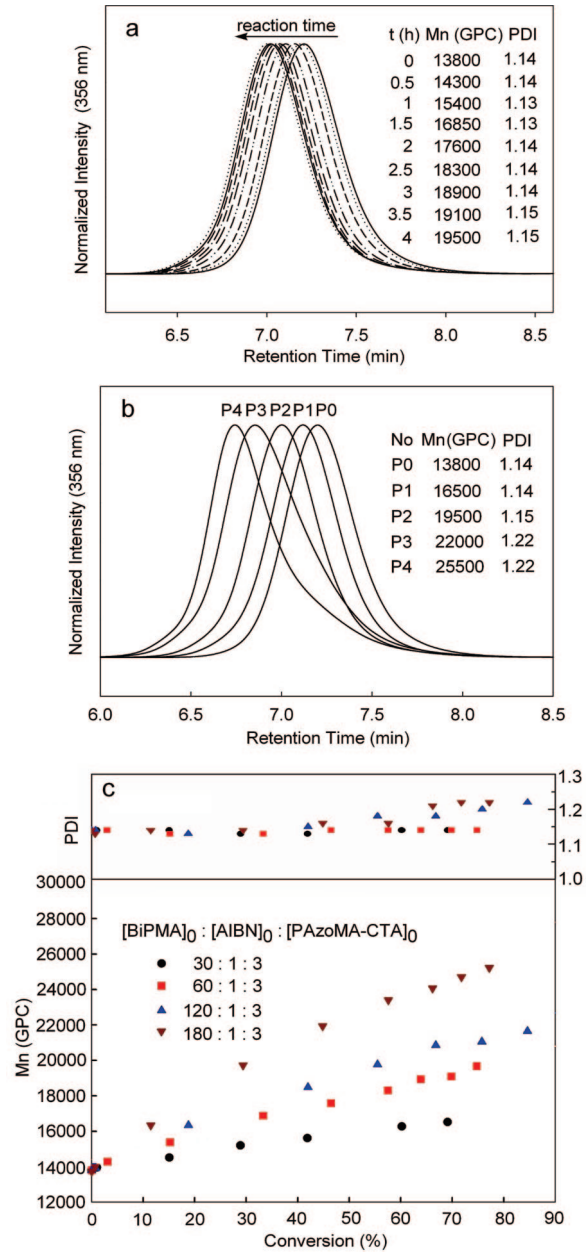

Figure 1. RAFT synthesis of PAzoMA-*b*-PBiPMA (using the same PAzoMA macromolecular chain transfer agent): (a) evolution of the GPC curve as a function of the reaction time at 75 °C at the molar feed ratio of [BiPMA]:[AIBN]:[PAzoMA-CTA] = 60:1:3; (b) GPC curves of the diblock copolymers obtained after 4 h reaction at different feed ratios, resulting in different PBiPMA block lengths; and (c) plots of the number-average molecular weight and polydispersity index (both from GPC) vs monomer (BiPMA) conversion for different feed ratios. RAFT = reversible addition−fragmentation chain transfer; PAzoMA-*b*-PBiPMA = diblock copolymer of 6-[4-(4-methoxyphenylazo)phenoxy]hexyl methacrylate (AzoMA) and 6-[4-(4-cyanophenyl)phenoxy]hexyl methacrylate (BiPMA); AIBN = 2,2′-azobis(isobutyronitrile); CTA = chain transfer agent; GPC = gel permeation chromatography.

PAzoMA-CTA or PBiPMA-CTA was used to estimate the number of monomeric units of the first block, and then the number of monomeric units of the second block was calculated according to the composition of the diblock copolymers as revealed by their ^{1}H NMR spectra, one example of which is shown in Figure 3 (P2 sample in Table 1). The relative amounts of phenyl protons of azobenzene and biphenyl groups can easily be obtained by comparing the integral (not shown) of the peak j of azobenzene with that of the peaks a, b, and c of biphenyl

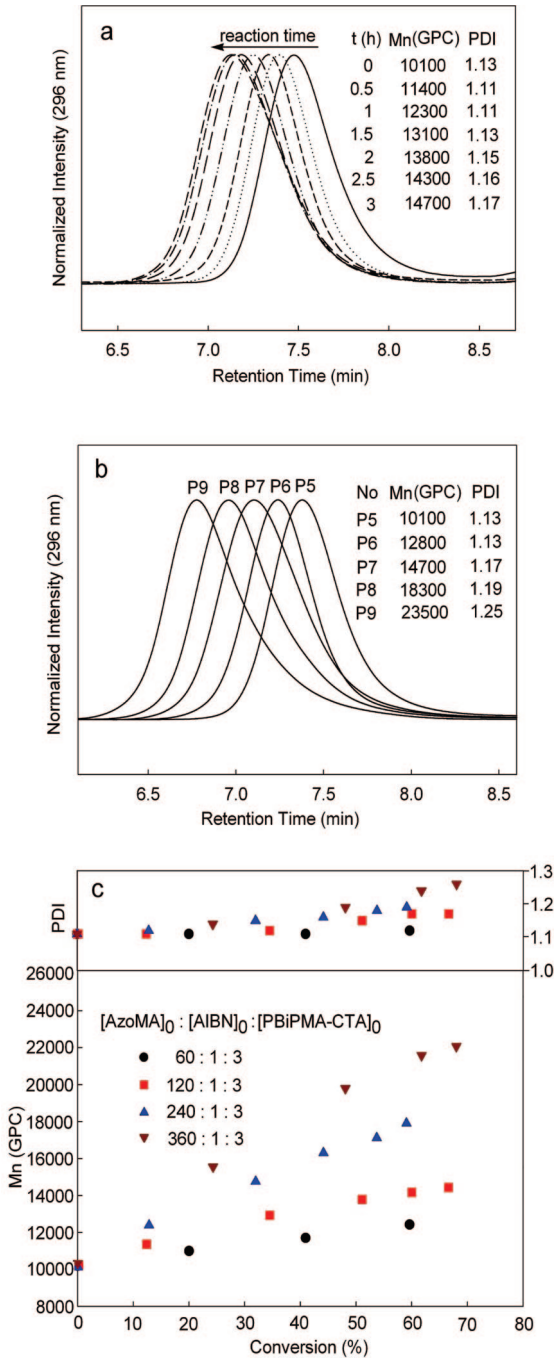

Figure 2. RAFT synthesis of PBiPMA-*b*-PAzoMA (using the same PBiPMA macromolecular chain transfer agent): (a) evolution of the GPC curve as a function of the reaction time at 75 °C at the molar feed ratio of [AzoMA]:[AIBN]:[PBiPMA-CTA] = 120:1:3; (b) GPC curves of the diblock copolymers obtained after 3 h reaction at different feed ratios, resulting in different PAzoMA block lengths; and (c) plots of the number-average molecular weight and polydispersity index (both from GPC) vs monomer (AzoMA) conversion for different feed ratios. RAFT = reversible addition−fragmentation chain transfer; PBiPMA-*b*-PAzoMA = diblock copolymer of 6-[4-(4-cyanophenyl)phenoxy-]hexyl methacrylate (BiPMA) and 6-[4-(4-methoxyphenylazo)phenox-y]hexyl methacrylate (AzoMA); AIBN = 2,2′- azobis(isobutyronitrile); CTA = chain transfer agent; GPC = gel permeation chromatography.

groups. Once the block copolymer compositions are determined, their molecular weights can be calculated. The results are also given in Table 1, labeled with M_n(NMR). It can be seen that M_n(NMR) is quite close to M_n(GPC) for most samples. M_n(NMR) becomes greater than M_n(GPC) with increasing the molecular weight of the second block, presumably due to the use of polystyrene standards for the calibration. It should be emphasized that that both M_n values are not the absolute molar mass and may contain significant errors. Despite the uncertainty about the absolute numbers of monomeric units, the block copolymer composition as revealed by ^{1}H NMR gives the relative lengths of the two blocks.

Table 1. Characteristics of Double Side-Chain Liquid Crystalline Block Polymers Synthesized by Reversible Addition−Fragmentation Chain Transfer Polymerization[a]

sample	composition	Azo (mol %)	$M_n \times 10^{-4}$ (GPC)	$M_n \times 10^{-4}$ (NMR)	PDI (GPC)
P0	$PAzoMA_{34}$-CTA	100	1.38		1.14
P1	$PAzoMA_{34}$-*b*-$PBiPMA_7$	83	1.65	1.62	1.15
P2	$PAzoMA_{34}$-*b*-$PBiPMA_{17}$	67	1.95	1.98	1.15
P3	$PAzoMA_{34}$-*b*-$PBiPMA_{36}$	49	2.20	2.67	1.22
P4	$PAzoMA_{34}$-*b*-$PBiPMA_{51}$	40	2.55	3.22	1.22
P5	$PBiPMA_{27}$-CTA	0	1.01		1.13
P6	$PBiPMA_{27}$-*b*-$PAzoMA_{11}$	29	1.28	1.44	1.13
P7	$PBiPMA_{27}$-*b*-$PAzoMA_{23}$	46	1.47	1.92	1.17
P8	$PBiPMA_{27}$-*b*-$PAzoMA_{38}$	58	1.83	2.51	1.19
P9	$PBiPMA_{27}$-*b*-$PAzoMA_{63}$	70	2.35	3.30	1.25

[a] PAzoMA-CTA = poly{6-[4-(4-methoxyphenylazo)phenoxy]hexyl methacrylate} chain transfer agent. PBiPMA-CTA = poly{6-[4-(4-cyanophenyl)phenoxy]hexyl methacrylate} chain transfer agent. PAzoMA-*b*-PBiPMA = diblock copolymer of 6-[4-(4-methoxyphenylazo)phenoxy-]hexyl methacrylate and 6-[4-(4-cyanophenyl)phenoxy]hexyl methacrylate synthesized using PAzoMA-CTA. PBiPMA-*b*-PAzoMA = diblock copolymer of 6-[4-(4-cyanophenyl)phenoxy]hexyl methacrylate and 6-[4-(4-methoxyphenylazo)phenoxy]hexyl methacrylate synthesized using PBiPMA-CTA (For each polymer or each polymer block, the subscript indicates the number of repeat units). M_n(GPC) = number-average molecular weight (g mol^{-1}) measured by gel permeation chromatography using polystyrene standards for calibration. M_n(NMR) = number-average molecular weight (g mol^{-1}) estimated by combining M_n(GPC) of the macromolecular chain transfer agent and the block copolymer composition determined by ^{1}H nuclear magnetic resonance comparing the intensity of azobenzene proton peak at 7.83 ppm to the intensity of the biphenyl proton peaks at 7.40−7.72 ppm. PDI (GPC) = polydispersity index defined as the ratio of weight-average molecular weight to number-average molecular weight measured by gel permeation chromatography using polystyrene standards for calibration.

The two series of diblock copolymers in Table 1 were characterized using a number of techniques. Figures 4 and 5 report the DSC heating and cooling curves (second scan). Before discussion, we mention that the LC phase behaviors of the homopolymers PAzoMA and PBiPMA are known in the literature.[22,23] Upon cooling from the isotropic phase, PAzoMA enters in a nematic phase over a wide temperature range before the transition into a smectic A phase at lower tempeartures.[22] As for PBiPMA, on cooling from the isotropic phase, it enters in a smectic A phase over a narrow temperature range followed by probably a smectic B phase, as indicated by a close exothermic shoulder on the DSC curve.[23] These LC mesophase transitions are observed for PAzoMA-CTA and PBiPMA-CTA in Figures 4 and 5, respectively. For the double SCLC block copolymers, some common features can be noticed. Starting with either of the SCLC macromolecular CTA, the linking of the second SCLCP changes drastically the mesophase transitions. For instance, upon heating $PAzoMA_{34}$-CTA displays a smectic-to-nematic and a nematic-to-isotropic phase transition endotherm at about 72 and 115 °C, respectively (Figure 4a), while with $PAzoMA_{34}$-*b*-$PBiPMA_7$, which contains the lowest content of PBiPMA among the series of diblock copolymers, the smectic-to-nematic transition peak can hardly be perceived. Upon further increase of the molar (thus volume) fraction of PBiPMA, apparently only the nematic-to-isotropic transition endotherm, shifted to higher temperatures around 130 °C, can be seen. And it is overlapped with a second peak, which likely arises from the smectic-to-isotropic phase transition of PBiPMA. The inclusion of two transitions in the broad peak is better revealed on the cooling curves displaying two exotherms, the overlap of which depends on the actual composition of the two

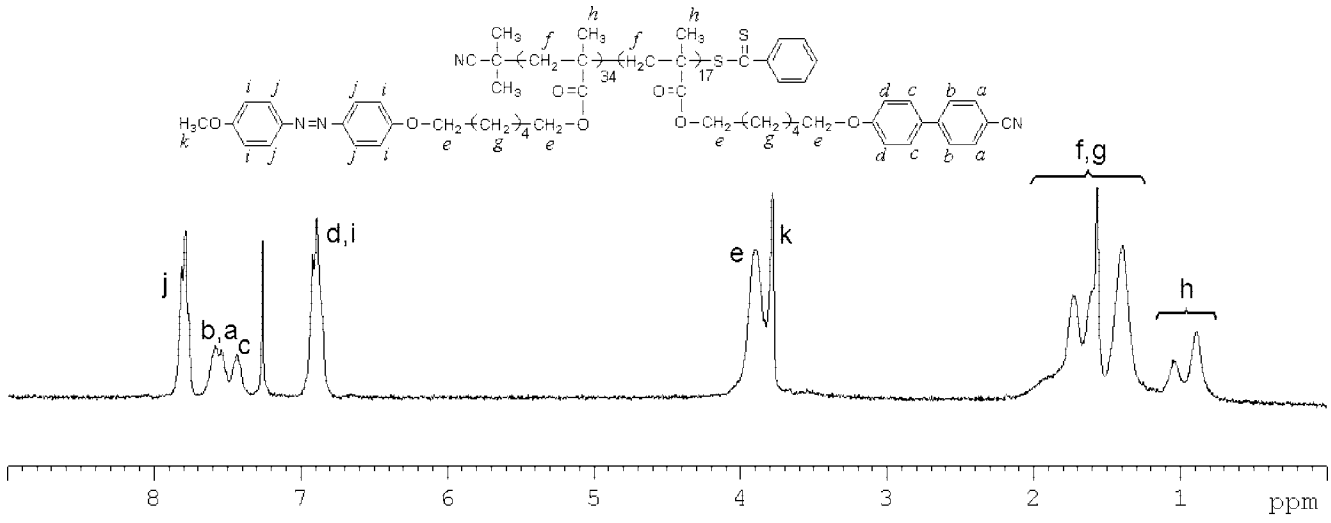

Figure 3. ^{1}H NMR spectrum (in $CDCl_3$) of the diblock copolymer $PAzoMA_{34}$-*b*-$PBiPMA_{17}$ synthesized by RAFT at 75 °C for 4 h, using $[BiPMA]_0$:$[AIBN]_0$:$[PAzoMA_{34}\text{-}CTA]_0$ = 60:1:3. RAFT = reversible addition−fragmentation chain transfer; PAzoMA-*b*-PBiPMA = diblock copolymer of 6-[4-(4-methoxyphenylazo)phenoxy]hexyl methacrylate (AzoMA) and 6-[4-(4-cyanophenyl)phenoxy]hexyl methacrylate (BiPMA); CTA = chain transfer agent.

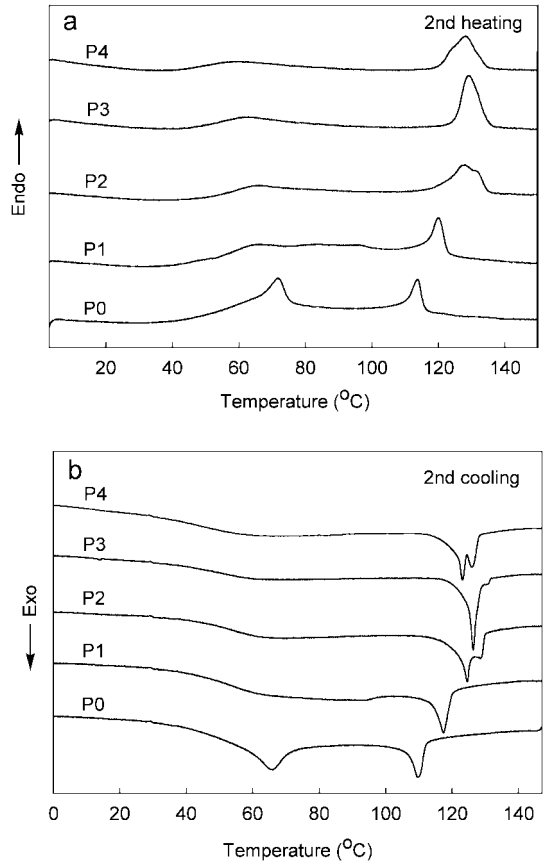

Figure 4. Differential scanning calorimetric heating and cooling curves for PAzoMA-*b*-PBiPMA diblock copolymers of various compositions (see Table 1 for details). PAzoMA-*b*-PBiPMA = diblock copolymer of 6-[4-(4-methoxyphenylazo)phenoxy]hexyl methacrylate (AzoMA) and 6-[4-(4-cyanophenyl)phenoxy]hexyl methacrylate (BiPMA).

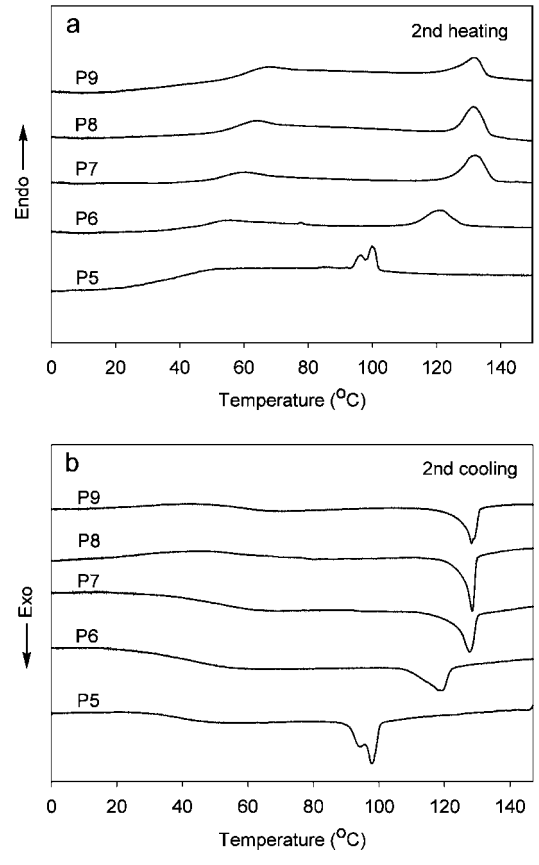

Figure 5. Differential scanning calorimetric heating and cooling curves for PBiPMA-*b*-PAzoMA diblock copolymers of various compositions (see Table 1 for details). PBiPMA-*b*-PAzoMA = diblock copolymer of 6-[4-(4-cyanophenyl)phenoxy]hexyl methacrylate (BiPMA) and 6-[4-(4-methoxyphenylazo)phenoxy]hexyl methacrylate (AzoMA).

SCLCPs (Figure 4b). Basically the same observations can be made for the series of samples prepared using the $PBiPMA_{27}$-CTA (Figure 5). The LC phase transition temperatures of PBiPMA are significantly increased by the presence of the PAzoMA block. For the samples containing high fractions of PAzoMA, the smectic-to-nematic transition becomes discernible at lower temperatures (∼65 °C). The results of DSC indicate that the LC phase transition behaviors in the double SCLC block copolymers are not the simple addition of the phase transitions of the two constituting SCLCP blocks. The low-temperature smectic phase of PAzoMA seems to be mostly disrupted by the diblock structure, while the main LC-to-isotropic phase transitions of the two blocks occur at significantly higher temperatures than when they were alone. This mutual enhancement in their LC phase thermal stability might be related to the

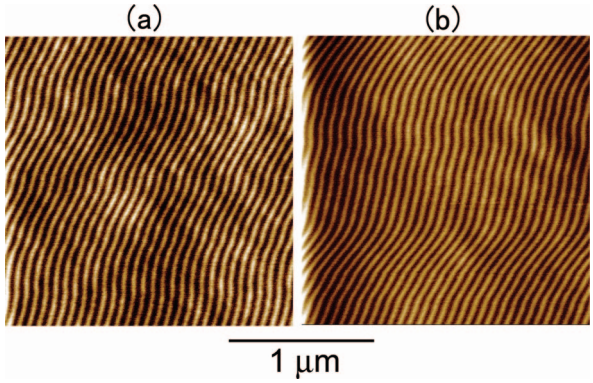

Figure 6. Atomic force microscope (AFM) phase images for (a) PAzoMA$_{34}$-*b*-PBiPMA$_{17}$ and (b) PAzoMA$_{34}$-*b*-PBiPMA$_{51}$. Image area: 2 μm × 2 μm. PAzoMA-*b*-PBiPMA = diblock copolymer of 6-[4-(4-methoxyphenylazo)phenoxy]hexyl methacrylate (AzoMA) and 6-[4-(4-cyanophenyl)phenoxy]hexyl methacrylate (BiPMA).

microphase-separated morphology and the anticipated cooperative effect on the ordering of the two mesogens through the large interface. In the present case, a more thorough and reliable analysis of the transition peaks (temperature and enthalpy) is difficult to do due to the fact that the two SCLCPs are of similar structures, both being polymethacrylates and having the same flexible spacer linking the backbone and the mesogenic side groups. Starting with either of the macromolecular CTA of a fixed molecular weight, the glass and LC phase transition temperatures of the second SCLCP block are function of the block length. In future studies, all-SCLC block copolymers can be designed with SCLCPs having very different T_g and LC phase transition temperatures, which should facilitate in-depth investigations of the two-level self-assembly and the interplay between different LC phases.

Despite the similar structures of the two SCLCPs, AFM measurements confirmed microphase-separated morphology for the diblock copolymers. Figure 6 shows the images obtained with P2 (PAzoMA$_{34}$-*b*-PBiPMA$_{17}$) and P4 (PAzoMA$_{34}$-*b*-PBiPMA$_{51}$). For the two samples, which differ in the relative amounts of the two blocks, a lamellar morphology is clearly visible on the phase image, with an estimated lamellar spacing of about 70 nm for both samples. We do not know which block is harder, corresponding to the white strips. POM observations also revealed the microphase-separated nature of the block copolymers. As an example, Figure 7 shows a series of micrographs for a film of P2 recorded upon cooling over a temperature range going through the broad exotherms on the DSC curve (Figure 4b). At each temperature the sample was held for 15 min for thermal equilibrium before the taking of the micrograph. The diblock copolymer is isotropic at 140 °C, appearing dark under crossed polarizers (photo not shown). The first isotropic-to-LC phase transition occurs at about 129 °C with the appearance of birefringent "batonnets" (photo a), which is indicative of a smectic A phase. This smectic A phase further developed at 127 °C, displaying the typical focal conic texture; however, the whole sample was not filled with the birefringent domains at this temperature (photo b). When the sample is further cooled to 125 °C, a second texture emerges and fills the sample. A closer look at this texture suggests the appearance of a nematic phase displaying threadlike defects or disclination lines (photo c). Upon further cooling to 123 °C, the second texture evolves and is superimposed with the smectic texture showing up at higher temperatures (photo d). Basically, such two distinct LC textures and the order of their appearance suggest the existence of two microphase-separated SCLCPs in the sample. Normally, if a SCLCP has a nematic and a smectic phase, on cooling from the isotropic phase, the nematic texture

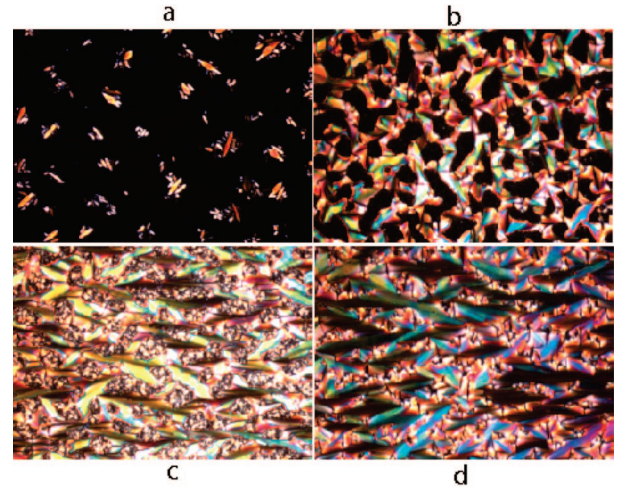

Figure 7. Polarizing optical micrographs of PAzoMA$_{34}$-*b*-PBiPMA$_{17}$ on cooling (~8 °C min^{-1}) from 140 °C (isotropic phase) to (a) 129, (b) 127, (c) 125, and (d) 123 °C (sample held at each temperature for 15 min before taking the micrograph). Image area: 180 μm × 130 μm. PAzoMA-*b*-PBiPMA = diblock copolymer of 6-[4-(4-methoxyphenylazo)phenoxy]hexyl methacrylate (AzoMA) and 6-[4-(4-cyanophenyl)phenoxy]hexyl methacrylate (BiPMA).

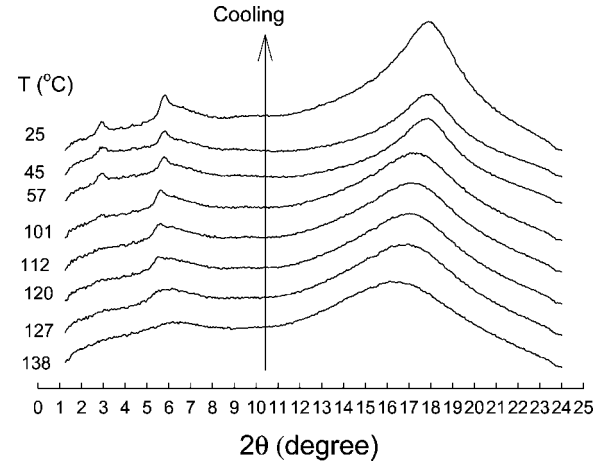

Figure 8. X-ray diffraction patterns of PAzoMA$_{34}$-*b*-PBiPMA$_{17}$ recorded at various temperatures on cooling from 140 °C to room temperature. PAzoMA-*b*-PBiPMA = diblock copolymer of 6-[4-(4-methoxyphenylazo)phenoxy]hexyl methacrylate (AzoMA) and 6-[4-(4-cyanophenyl)phenoxy]hexyl methacrylate (BiPMA).

should be observed first, followed by its transformation onto the smectic texture at lower temperatures. Considering the fact that on cooling the PAzoMA homopolymer has a nematic phase over a wide temperatures range,[22] while PBiPMA has only smectic phases,[23] the first smectic texture observed on cooling of P2 is likely to come from PBiPMA, followed by PAzoMA entering its nematic phase. It is difficult to tell whether PAzoMA has a smectic phase at lower temperatures from POM due to the overlap of the two textures.

X-ray diffraction measurements were carried out with the P2 sample upon cooling from the isotropic phase (140 °C) to room temperature (25 °C). Figure 8 shows the diffraction profiles for selected temperatures, at each of which the sample was held for 10 min for equilibrium prior to the measurement. Apart from the usual broad diffraction halo at $2\Theta \approx 18°$ related to the disordered lateral arrangement of mesogens and polymer chains, the appearance of a smectic phase can be seen from small-angle diffraction peaks. At 120 °C, a weak peak at $2\Theta = 5.5°$ becomes visible, which should arise from the smectic phase of the PBiPMA block. On further cooling to 57° another small-angle

diffraction peak appears at $2\Theta = 3.0°$, while the first peak shifts to ~5.9°. Since they have the reciprocal spacing in the 1:2 ratio, they are likely the first- and second-order diffractions from the same lamellar packing structure of PBiPMA. On closer inspection, the diffraction peak at $2\Theta \approx 3°$ is discernible at 101 °C, where PAzoMA could not be in the smectic phase. Indeed, under the same conditions, no small-angle diffraction peaks could be detected for PAzoMA-CTA (the homopolymer). Therefore, the result in Figure 8 suggests that on cooling only the PBiPMA block could form the smectic phase inside the lamellar domains (Figure 6). The layer spacing calculated from the first-order diffraction peak is $d = 29.5$ Å, which is larger than the total length of the side-chain estimated to be $L = 23$ Å (biphenyl mesogen plus the spacer with extended conformation). The ratio of $d/L = 1.28$ indicates a partially interdigitated smectic (S_{Ad}) phase of PBiPMA, which indeed is known for cyanobiphenyl-based SCLCPs.[23] A couple of additional notes are worth being made. First, the small-angle diffraction peaks are very weak, suggesting that the smectic ordering be difficult to develop. Second, the first-order diffraction is weaker than the second-order diffraction, which is uncommon but has been reported for a number of SCLCPs.[24–26]

2. Orientational Cooperative Effect. In the case of SCLC random copolymers whose chain backbone bears two different side groups, one of which is azobenzene mesogen, the orientational cooperative effect is easily observable.[27] That is, the photoinduced orientation of azobenzene mesogens under linearly polarized irradiation can bring the non-azobenzene mesogens to align with them. Recently, Yu et al. also demonstrated this cooperative effect under confinement by using a block copolymer whose microphase-separated morphology consisted in a poly(methyl methacrylate) (PMMA) matrix with dispersed spherical microdomains formed by two SCLCP blocks containing azobenzene and nonazobenzene mesogens, respectively.[28] Inside the spherical microdomains (20−80 nm in diameter) no segregation of the two SCLCPs was evidenced. In fact, the block copolymer, synthesized with ATRP using PMMA-Br macroinitiator, has a very short block of the azobenzene-containing SCLCP with only five monomer units, and the two types of mesogens are likely to be mixed inside the spherical microdomains. A question of fundamental interest is whether or not the orientational cooperative effect is significant between two microphase-separated SCLCPs. In other words, can the photoinduced orientation of azobenzene mesogens confined in one microphase induce an orientation of the nonazobenzene mesogens located inside their own microdomains via the interface where the two types of mesogens encounter? We investigated this using the P2 and P4 samples, i.e., $PAzoMA_{34}$-*b*-$PBiPMA_{17}$ and $PAzoMA_{34}$-*b*-$PBiPMA_{51}$, whose lamellar microphase-separated morphology was evidenced by AFM (Figure 6).

To discuss the orientational cooperative effect, the UV−vis spectra of the series of samples with the same $PAzoMA_{34}$ block (P0−P4) are first shown in Figure 9a. With respect to the absorption of trans azobenzene peaked at ~360 nm, the absorption peak of biphenyl mesogens at 296 nm becomes more and more prominent with increasing the amount of the PBiPMA block. It can be seen that *trans*-azobenzene has very small absorption around 290 nm. Moreover, the absorption peaks of azobenzene of all diblock copolymers appear to be the same as the PAzoMA homopolymer, suggesting that the azobenzene mesogens have similar aggregation states in all samples.[12,29] Using P4 as an example, Figure 9b shows the effective photoisomerization, and the resulting long-range orientation of azobenzene mesogens that can take place upon UV and visible light irradiation. The photoinduced orientation of azobenzene mesogens in the thin film was achieved using a known method.[12,30] It consists of using first unpolarized UV light to

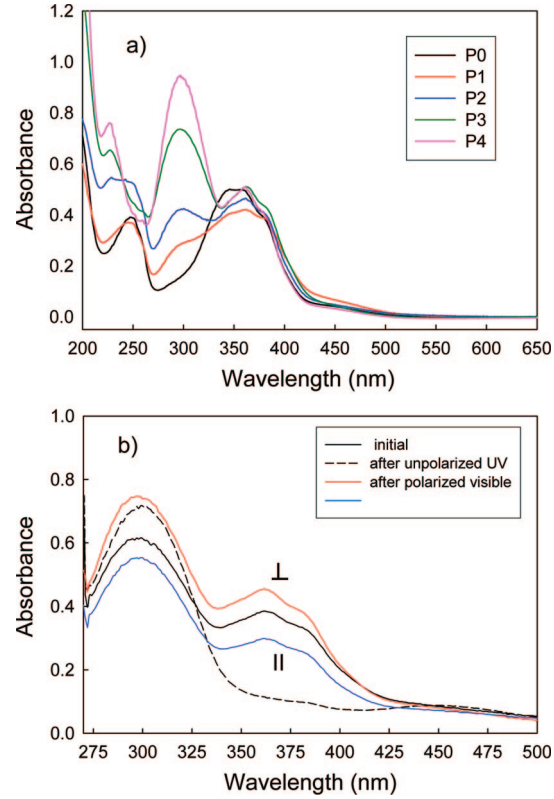

Figure 9. (a) UV−vis spectra of PAzoMA homopolymer and PAzoMA-*b*-PBiPMA diblock copolymers of various compositions. (b) UV−vis spectra of $PAzoMA_{34}$-*b*-$PBiPMA_{51}$ before and after unpolarized UV irradiation (85 mW cm^{-2}, 10 min) as well as the polarized spectra recorded after subsequent linearly polarized visible light irradiation (5 mW cm^{-2}, 15 min). The photoinduced orientation of azobenzene mesogenic groups on the PAzoMA block is indicated by the perpendicular dichroism of the absorption at 360 nm, while the liquid crystalline cooperative effect-induced orientation of biphenyl mesogenic groups on the PBiPMA block is revealed by the dichroism of the absorption around 296 nm (see text for details). PAzoMA = poly{6-[4-(4-methoxyphenylazo)phenoxy]hexyl methacrylate}; PAzoMA-*b*-PBiPMA = diblock copolymer of 6-[4-(4-methoxyphenylazo)phenoxy]hexyl methacrylate (AzoMA) and 6-[4-(4-cyanophenyl)phenoxy]hexyl methacrylate (BiPMA).

convert *trans*-azobenzene onto the cis isomer and then applying linearly polarized visible light to induce the cis−trans back-isomerization and the concurrent orientation of azobenzene mesogens in the direction perpendicular to the polarization of the visible light. Upon unpolarized UV irradiation leading to the photostationary state (85 mW cm^{-2} for 10 min), the absorption of *trans*-azobenzene around 360 nm basically disappears as a result of the nearly complete trans−cis photoisomerization (with more than 90% of trans azobenzene converted to the cis isomer). Upon subsequent linearly polarized visible light irradiation (5 mW cm^{-2} for 15 min), the absorption of *trans*-azobenzene is largely recovered indicating the conversion of cis isomer to the trans form. Shown in Figure 9b are the polarized UV−vis spectra of the film recorded with the spectrophotometer's beam polarized parallely and perpendicularly to the polarization direction of the visible light. Indeed, the absorption peak of trans azobenzene at 360 nm displays a perpendicular dichroism indicating the photoinduced orientation of azobenzene mesogens in the expected direction. Interestingly, the absorption peak of biphenyl groups at ~296 nm also shows a clear but smaller dichroism in the same direction. Considering the slight overlap of the absorption peaks of azobenzene and biphenyl groups, the order parameters of the two mesogens can easily be calculated according to $S = (A_\perp/A_\parallel - 1)/(A_\perp/A_\parallel + 2)$, using the perpendicular ($A_\perp$) and parallel absorbance ($A_\parallel$) of the

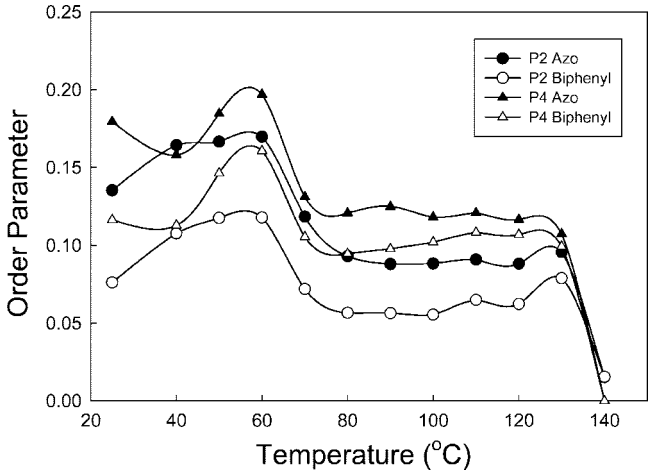

Figure 10. Plots of order parameter vs annealing temperature that shows the change in orientation for both azobenzene and biphenyl mesogenic groups in films of $PAzoMA_{34}$-*b*-$PBiPMA_{17}$ (P2) and $PAzoMA_{34}$-*b*-$PBiPMA_{51}$ (P4) upon the thermal annealing following the unpolarized UV and linearly polarized visible light irradiation. PAzoMA-*b*-PBiPMA = diblock copolymer of 6-[4-(4-methoxyphenylazo)phenoxy]hexyl methacrylate (AzoMA) and 6-[4-(4-cyanophenyl)phenoxy]hexyl methacrylate (BiPMA).

peaks at 360 and 296 nm, respectively. For this P4 film, azobenzene groups have $S = 0.18$ while biphenyl groups have $S = 0.12$. This result clearly shows that despite the microphase-separated lamellar morphology, the photoinduced orientation of azobenzene mesogens in one domain can bring biphenyl mesogens located in their own domain to orient in the same direction. This orientational cooperative effect should stem from the LC nature of the two polymers. Actually, PBiPMA has a low T_g around room temperature, which likely enables the propagation of orientation from azobenzene to biphenyl mesogenic groups via the large interface associated with the microphase-separated morphology. In the interfacial region, some mixing of the two types of mesogenic groups, those close to the linkage of the two blocks, should be expected. Nevertheless, considering that the order parameter measures the average orientation of all mesogenic groups, the similar orientational degree for the two mesogens implies that the orientation of biphenyl groups induced by the photoorientation of azobenzene groups did not occur solely in the interfacial region; rather, it took place inside the lamellar domains of PBiPMA.

In a previous study on a diblock copolymer composed of polystyrene (PS) and the same azobenzene-containing SCLCP (PS-*b*-PAzoMA),[12] thermal annealing of photoaligned films in the LC phases of PAzoMA resulted in an increase of the orientation of azobenzene mesogens due to their enhanced self-organization and ordering. To see how the change in the orientation of PAzoMA upon thermal annealing could affect the orientation of biphenyl groups in their own microphase, P2 and P4 films after the photoinduced orientation were subjected to thermal annealing at various temperatures (10 min at a given temperature by placing the film in a preheated oven), and the polarized UV−vis spectra were taken after cooling the films to room temperature. Figure 10 shows the plots of order parameter as a function of annealing temperature for both mesogenic groups and in both P2 and P4 films. A similar trend for the change in the orientation degree is observed for the two block copolymers. The highest orientation of azobenzene is observed at ~60 °C, just above T_g of PAzoMA, where the chain backbone mobility apparently enhances the self-ordering of azobenzene groups in their LC phase. This thermally induced increase in orientation of azobenzene is accompanied by an increase of the orientation of biphenyl groups, which further confirms the effective orientational cooperative effect in microphase-separated double SCLC block copolymers. Upon further heating to $T >$ 60 °C, the orientation of azobenzene decreases, and so does the orientation of biphenyl groups. This change is likely to be related to the transformation of the LC phase of PAzoMA at $T <$ 60 °C to a less ordered mesophase at the higher temperatures. This behavior is compatible with that PAzoMA displays a smectic phase in a temperature range close to T_g and a wide-range nematic phase before the isotropization, as mentioned earlier (Figure 4). This result suggests the existence of a smectic phase at lower temperatures for PAzoMA in the block copolymers (at least smectic ordering of azobenzene groups) even though it could not be clearly revealed by the characterization techniques used. For both P2 and P4, over the range of annealing temperatures, the orientation of biphenyl groups remains smaller than the orientation of azobenzene groups. At 140 °C in the isotropic phase, it is no surprise that the orientation of the two mesogens is gone.

Conclusions

We reported the RAFT synthesis and characterization of the first diblock copolymer composed of two SCLCPs, one of which contains azobenzene mesogenic groups. We demonstrated the efficiency of RAFT in preparing this new type of block copolymer. The studied PAzoMA-*b*-PBiPMA could be obtained using either PAzoMA-CTA to grow the PBiPMA block or, reversely, using PBiPMA-CTA to grow the PAzoMA block. In both ways, copolymers of various compositions with low polydispersity were obtained. Using the double SCLC diblock copolymer, we investigated the orientational cooperative effect between the two microphase-separated SCLCPs. We found that the photoinduced orientation of azobenzene mesogens of PAzoMA could propagate into the microphase-segregated PBiPMA domains through the interface, resulting in an orientation of the biphenyl mesogens of PBiPMA in the same direction. This study shows that double or all-SCLC copolymers can be designed and synthesized by RAFT, which might exhibit new interplay effects and competition behaviors involving the microphase-separation-induced morphology and the LC ordering of different SCLCPs.

Acknowledgment. We acknowledge the financial support from the Natural Sciences and Engineering Research Council of Canada (NSERC) and le Fonds québécois de la recherche sur la nature et les technologies of Québec (FQRNT). We also thank Prof. Geraldine Bazuin, Mr. Sylvain Essiembre, and Mr. Qian Zhang (University of Montreal) for helpful discussions and assistance with the X-ray diffraction measurements. Y.Z. is a member of the FQRNT-funded Center for Self-Assembled Chemical Structures.

References and Notes

(1) Fischer, H.; Poser, S.; Arnold, M.; Frank, W. *Macromolecules* **1994**, *27*, 67133–7138.
(2) Wong, G. C. L.; Commandeur, J.; Fischer, H.; de Jeu, W. H. *Phys. Rev. Lett.* **1996**, *77*, 5221–5224.
(3) Sanger, J.; Gronski, W.; Maas, S.; Stuhn, B.; Heck, B. *Macromolecules* **1997**, *30*, 6783–6787.
(4) Mao, G.; Wang, J.; Clingman, S. R.; Ober, C. K.; Chen, J.; Thomas, E. L. *Macromolecules* **1997**, *30*, 2556–2567.
(5) Yamada, M.; Igushi, T.; Hirao, A.; Nakahama, S.; Watanabe, J. *Polym. J.* **1998**, *30*, 23–30.
(6) Zheng, W. Y.; Albaluk, R. J.; Hammond, P. T. *Macromolecules* **1998**, *31*, 2686–2689.
(7) Anthamatten, M.; Zhang, W. Y.; Hammond, P. T. *Macromolecules* **1999**, *32*, 4838–4848.
(8) Schneider, A.; Zanna, J.-J.; Yamada, M.; Finkelmann, H.; Thomann, R. *Macromolecules* **2000**, *33*, 649–651.
(9) Li, M.-H.; Keller, P.; Albouy, P.-A. *Macromolecules* **2003**, *36*, 2284–2292.

(10) Hamley, I. W.; Castelletto, V.; Parras, P.; Lu, Z. B.; Imrie, T.; Itoh, T. *Soft Matter* **2005**, *1*, 355–363.
(11) Verploegen, E.; MacAfee, L. C.; Tian, L.; Verploegen, D.; Hammond, P. T. *Macromolecules* **2007**, *40*, 777–780.
(12) Tong, X.; Cui, L.; Zhao, Y. *Macromolecules* **2004**, *37*, 3101–3112.
(13) Yu, H. F.; Iyoda, T.; Ikeda, T. *J. Am. Chem. Soc.* **2006**, *128*, 11010–11011.
(14) Cui, L.; Zhao, Y.; Yavrian, A.; Galstian, T. *Macromolecules* **2003**, *36*, 8246–8252.
(15) Han, Y.-K.; Dufour, B.; Wu, W.; Kowalewski, T.; Matyjaszewski, K. *Macromolecules* **2004**, *37*, 9355–9365.
(16) Sin, S. H.; Gan, L. H.; Hu, X.; Tam, K. C.; Gan, Y. Y. *Macromolecules* **2005**, *38*, 3943–3948.
(17) Su, W.; Zhao, H. *Eur. Polym. J.* **2007**, *43*, 657–662.
(18) Zhang, Y.; Cheng, Z.; Chen, X.; Zhang, W.; Wu, J.; Zhu, J.; Zhu, X. *Macromolecules* **2007**, *40*, 4809–4817.
(19) Ringsdorf, H.; Schmidt, H. W. *Makromol. Chem.* **1984**, *185*, 1327–1334.
(20) Portugall, M.; Ringsdorf, H.; Zentel, R. *Makromol. Chem.* **1982**, *183*, 2311–2321.
(21) Song, J. S.; Winnik, M. A. *Macromolecules* **2006**, *39*, 8318–8325.
(22) Walther, M.; Faulhammer, H.; Finkelmann, H. *Macromol. Chem. Phys.* **1998**, *199*, 223–237.
(23) Craig, A. A.; Imrie, C. T. *Macromolecules* **1995**, *28*, 3617–3624.
(24) Masson, P.; Gramain, P. H.; Guillon, D. *Macromol. Chem. Phys.* **1995**, *196*, 3677–3686.
(25) Tibirna, C. M.; Bazuin, G. *J. Polym. Sci., Polym. Phys.* **2005**, *43*, 3421–3431.
(26) Li, M.-H.; Keller, P.; Grelet, E.; Auroy, P. *Macromol. Chem. Phys.* **2002**, *203*, 619.
(27) Ikeda, T. *J. Mater. Chem.* **2003**, *13*, 2037–2057.
(28) Yu, H.; Asaoka, S.; Shishido, A.; Iyoda, T.; Ikeda, T. *Small* **2007**, *5*, 768–771.
(29) Deng, Y. H.; Li, Y. B.; Wang, X. G. *Macromolecules* **2006**, *39*, 6590–6598.
(30) Wu, Y.; Zhang, Q.; Kanazawa, A.; Shiono, T.; Ikeda, T.; Nagase, Y. *Macromolecules* **1999**, *32*, 3951–3956.

MA8000302